

Statistical Properties of the Poly(*N*-vinylcarbazole) Chain As Estimated from an NMR Analysis of 2,4-Bis-*N*-carbazolylpentane

Akihiro Abe* and Hideyuki Kobayashi

Department of Polymer Chemistry, Tokyo Institute of Technology, Okayama, Meguro-ku, Tokyo 152, Japan

Tokiji Kawamura

Department of Industrial Chemistry, Faculty of Engineering, University of Tokyo, Hongo, Bunkyo-ku, Tokyo 113, Japan

Masazumi Date and Toshiyuki Uryu

Institute of Industrial Science, University of Tokyo, Roppongi, Minato-ku, Tokyo 106, Japan

Kei Matsuzaki

Faculty of Textile Science and Technology, Shinshu University, Ueda 386, Japan.
Received February 24, 1988; Revised Manuscript Received April 13, 1988

ABSTRACT: Samples of *meso*- and *rac*-2,4-bis-*N*-carbazolylpentane were prepared in high purity by the reaction of 2,4-di-*O*-tosylpentane or 2,4-di-*O*-mesylpentane with carbazolyl potassium. NMR ^1H - ^1H vicinal coupling constants and their temperature dependence were measured. Statistical weight parameters, and thus conformational energies, estimated therefrom were used to elucidate the conformational characteristics of the poly(*N*-vinylcarbazole) (PVK) chain. Experimental values of the characteristic ratios for the unperturbed dimension $\langle r^2 \rangle_0/nl^2 = 15$ -19 and the dipole moment $\langle \mu^2 \rangle/xm^2 = 0.3$ -0.5 were found to be reasonably reproduced by the calculation for moderately syndiotactic chains. Fractions of the *tt* conformation were estimated for the *meso* and *racemo* diads incorporated in PVK chains: at $P_{\text{iso}} = 0.5$, $f_{\text{tt},\text{m}} = 0$ -0.05 and $f_{\text{tt},\text{r}} = 0.43$ -0.47. In the ground state, the so-called "sandwich structure" (*meso*-*tt*) is a rare occurrence. Configurational statistics of the polymer chain may be quite different in the excited state, where formation of the *meso*-*tt* form is reported to be very rapid. The conformational energy parameter sets proposed by the other research groups were found to overestimate the *meso*-*tt* state to a considerable degree.

Introduction

Poly(*N*-vinylcarbazole) (PVK) has been a subject of various investigations mainly because of its unique photochemical properties. Stereochemical configuration of the polymer has been studied by the NMR method.¹⁻¹¹ Terrel and Evers⁹ attempted to elucidate the triad fraction from the ^{13}C NMR spectra of the methine group for radically polymerized PVKs. The fraction of the isotactic diad sequence, $P_{\text{iso}} = 1 - P_{\text{syndio}}$, was estimated to be in the range 0.25-0.47. They also reported dyad tacticities for some cationically polymerized samples:¹⁰ $P_{\text{iso}} = 0.32$ -0.57 (by ^1H NMR) and 0.37-0.52 (by ^{13}C NMR). In order to establish a refined peak assignment, Kawamura et al.¹¹ prepared partially deuterated PVK samples (poly(*N*-vinylcarbazole- β,β - d_2)). The dyad tacticity was found to be ca. 0.5 for the radical process. Higher isotactic fractions ($P_{\text{iso}} = 0.5$ -0.7) were obtained for polymers prepared with a cationic initiator.

Several studies have been reported for solution properties of PVK. The experimental values of the characteristic ratio of the unperturbed dimension $\langle r^2 \rangle_0/nl^2$, n being the number of skeletal bonds and l the C-C bond length, were estimated to be 16.9¹² and 17.7¹³ for radically prepared PVKs and 15.4¹⁴ and 19.0¹⁵ for cationically polymerized samples. In these treatments, the viscosity constant¹⁶ $\Phi = 2.6 \times 10^{23}$ was consistently adopted. The dipole moment of the polymer has been measured in nonpolar solvents such as 1,4-dioxane and toluene. The dipole moment ratio $\langle \mu^2 \rangle/xm^2$, $x = n/2$ being the number of monomer residues and m the dipole moment of the repeating unit, was reported to be 0.33,¹⁷ 0.41,¹⁸ 0.42,¹⁹ and 0.50,²⁰ all samples being radically prepared. Here following Molina et al.,¹⁸ the value of m was taken from North and

Phillips' work²⁰ on *N*-isopropylcarbazole (2.96 D).²¹ A somewhat higher value (0.53 D) was observed for a cationically prepared PVK.¹⁷

Conformational energy maps for the internal bond rotation were estimated by Sundararajan,²² who employed conventional semiempirical energy expressions to calculate short-range steric interactions, the coulombic interaction terms being ignored. Conformational energies thus estimated were found to vary rather sensitively to the cut-off distance of the pairwise interaction. The bulkiness of the side groups prevents an unambiguous estimation of the conformational energies. The calculation of $\langle r^2 \rangle_0/nl^2$ was performed for various values of the energy parameters. Through comparison with experimental observations, Sundararajan deduced a probable set of conformational energy parameters. The same energy parameters were adopted in the calculation of $\langle \mu^2 \rangle/xm^2$ by Molina et al.¹⁸ Privratska and Havranek²³ also estimated energy contour maps for PVK by using semiempirical energy functions. The conformational energy parameter set prescribed on this basis is quite different from those given by Sundararajan²² (cf. the following).

^1H NMR studies on the dimer model compound of PVK, 2,4-bis-*N*-carbazolylpentane (BCP), have been reported by De Schryver et al.,²⁴ Vandendriessche et al.,²⁵ and Evers et al.²⁶ The former authors determined vicinal coupling constants, $^3J_{\text{HH}}$, for the methylene and methine protons. For a sample of *meso*-BCP with a moderate purity (>80%), they obtained $J_{\text{AX}} \simeq J_{\text{BX}}$. A similar observation has been reported for *meso*-2,4-diphenylpentane by Bovey et al.²⁷ De Schryver and co-workers^{24,25} concluded on this basis that the *tg* (or *gt*) conformation was the only existing species (100%) in solution. As shown by a simple ma-

Table I
¹H NMR Data of *meso*-BCP in Acetone-*d*₆ and Chloroform-*d*

solvent	temp, °C	H _A , ppm	H _B , ppm	H _X , ppm	J _{AB} , Hz	J _{AX} , Hz	J _{BX} , Hz
(CD ₃) ₂ CO	50	3.01	3.03	4.76	-14.31	7.29	7.51
(CD ₃) ₂ CO	10	2.99	3.03	4.72	-14.12	7.72	7.85
(CD ₃) ₂ CO	-30	2.94	3.05	4.68	-14.12	7.71	7.96
(CD ₃) ₂ CO	-70	2.87	3.01	4.60	-13.91	7.64	7.85
CDCl ₃	50	2.84	3.04	4.65	-14.47	7.60	7.62
CDCl ₃	30	2.88	3.05	4.66	-14.27	7.77	7.79
CDCl ₃	10	2.88	3.02	4.65	-14.61	7.61	7.65
CDCl ₃	-30	2.90	2.99	4.64	-14.61	7.58	7.67
CDCl ₃	-50	2.92	2.98	4.64	-14.42	7.80	7.72

Table II
¹H NMR Data of *rac*-BCP in Acetone-*d*₆ and Chloroform-*d*

solvent	temp, °C	H _A , ppm	H _{A'} , ppm	H _X , ppm	J _{AA'} , Hz	J _{AX} , Hz	J _{A'X} , Hz
(CD ₃) ₂ CO	50	3.10	3.10	4.53	-14.92	10.28	4.98
(CD ₃) ₂ CO	10	3.14	3.14	4.55	-15.20	10.17	4.81
(CD ₃) ₂ CO	-30	3.12	3.12	4.52	-14.84	10.28	4.98
CDCl ₃	50	3.06	3.06	4.42	-14.47	10.94	4.46
CDCl ₃	30	3.08	3.08	4.42	-14.75	11.18	4.49
CDCl ₃	10	3.08	3.08	4.40	-14.80	10.89	4.37
CDCl ₃	-10	3.09	3.09	4.33	-14.79	11.17	4.47
CDCl ₃	-50	3.09	3.09	4.37	-15.08	10.73	4.83

nipulation, however, the calculation using the statistical weight parameter set of Sundararajan²² yields a considerable fraction (10%) of *meso*-tt, being inconsistent with the conclusion drawn by De Schryver and co-workers.^{24,25} Privratska and Havranek²³ predicted a much higher fraction (66%) for the same conformer from their conformational energy calculations. From the NMR analysis on *rac*-BCP (purity, >95%), De Schryver and co-workers^{24,25} found that the dominant contributors were the tt and/or gg conformation: from supplemental information for the chemical shift of the ring protons, the authors suggested that the former (tt) was more stable than the latter (gg). Sundararajan's parameter set²² yields populations of tt (70%) and gg (11%) in the correct order, but a fraction of 19% is assigned to tg + gt, which is again incompatible with the conclusions of De Schryver and co-workers.^{24,25} In contrast, Privratska and Havranek²³ attributed the entire fraction to the tt conformer in *rac*-BCP.

In view of these divergencies among various approaches, we have attempted in this work to establish reliable values of the statistical weight parameters from the NMR studies of the dimer model compounds. Highly purified samples of *meso*- and *rac*-BCP were prepared by the reaction of 2,4-di-*O*-tosylpentane or 2,4-di-*O*-mesylpentane with carbazoyl potassium. NMR ¹H-¹H vicinal coupling constants and their temperature dependence were measured. The statistical weight parameters, and thus the conformational energies, were estimated by the rotational isomeric state (RIS) analysis. Various conformation-dependent properties of the PVK chain were calculated, and the results were found to be favorably compared with those observed.

Experimental Section

Synthesis. *meso*-2,4-Bis-*N*-carbazoylpentane (*meso*-BCP). 2,4-Di-*O*-tosylpentane (I) was prepared from 2,4-pentadiol (*meso*/racemo = 43/57) and tosyl chloride by a conventional method. Aqueous potassium hydroxide solution (66%, 15 mL) was added to a mixture of I (10 g) and carbazole (14 g) dissolved in acetone (150 mL). After being refluxed for 5–12 h, the solution was poured into water. The precipitate formed was filtered, dried in vacuo, and recrystallized from ethanol. The reaction yielded only *meso*-BCP, regardless of the composition (*meso*/racemo) of the starting mixture. For example, when *rac*-I was used as the starting material, *N*-ethylcarbazole was obtained as the main product, *meso*-BCP being formed only in a trace amount.

rac-2,4-Bis-*N*-carbazoylpentane (*rac*-BCP). 2,4-Di-*O*-mesylpentane (II) was obtained from 2,4-pentadiol by reacting it with mesyl chloride. Aqueous potassium hydroxide solution (66%, 16 mL) was added to carbazole (16 g) dissolved in acetone (150 mL), and the mixture was refluxed for 1 h. Then II (*meso*/racemo = 43/57) (10 g) dissolved in acetone (50 mL) was added dropwise, and the solution was kept standing for 6 h. Then the solution was poured into water, and the precipitate was extracted with benzene. The extract was separated into four fractions with a TLC (Merck Art. 5717 with benzene/hexane (1/1) used as eluent): *R*_f = 0.25 (carbazole), 0.52 (*meso*-BCP), 0.61 (*rac*-BCP), 0.83 (*N*-ethylcarbazole). The carbazoylation reaction of II yielded *meso*- and *rac*-BCP in a ratio 7/3 even when *rac*-II was used as the starting material.

NMR Spectroscopy. ¹H NMR measurements were carried out on a JNM GX-400 NMR spectrometer operating at 399.85 MHz between -50 and 50 °C. ¹³C NMR measurements were performed on the same apparatus operating at 100.40 MHz between -30 and 25 °C on samples (500 mg) dissolved in CDCl₃ (5 mL). Tetramethylsilane was used as an internal reference in both measurements. The gated nondecoupling with the NOE method was used to determine *J*_{CH} coupling constants: repetition time, 2.000 s; 45° pulse, 4.5 μs; pulse delay, 1.000 s; acquisition time, 0.819 s; data points, 32768; scans, 40000.

Results and Discussion

Examples of the methine and methylene proton spectra are shown in Figure 1. In *meso*-BCP, the two methylene protons are sterically nonequivalent, and accordingly the signals appear at different chemical shifts. The methylene spectra were analyzed by using the LAOCOON III program assuming spin systems ABX₂ for the *meso* and AA'XX' for the racemo compound. Values of the observed chemical shifts and the geminal and vicinal coupling constants obtained by the analysis are listed in Tables I and II, respectively, for *meso*- and *rac*-BCP. The ¹H NMR measurements were carried out in two solvents, CDCl₃ and acetone-*d*₆. As indicated in these tables, the temperature dependence of vicinal coupling constants is relatively small. The vicinal coupling constants observed in CDCl₃ are close to those obtained in CD₂Cl₂ at 300 K.²⁴

The carbazole ring protons exhibit nonequivalent chemical shifts at low temperatures. The observed splittings are larger in *rac*-BCP than in *meso*-BCP. As pointed out by De Schryver and co-workers,^{24,25} these differences probably arise from the disparity in the spatial correlation of the two chromophores of the dimer. The coalescence of the ring proton spectra was observed at ca. 10 °C for

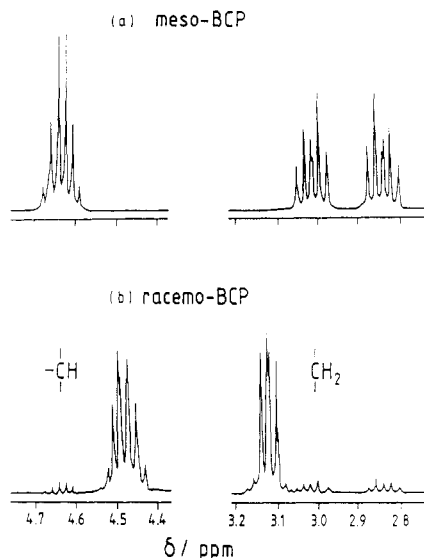


Figure 1. ^1H NMR spectra (400 MHz) of methine and methylene protons, measured in CDCl_3 at room temperature: (a) *meso*-BCP and (b) *rac*-BCP.

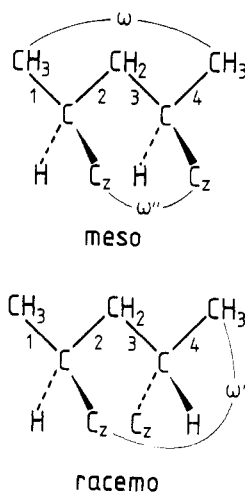


Figure 2. Schematic diagram of *meso*- and *rac*-BCP. The second-order interactions required in the RIS treatment are indicated.

meso-BCP and at ca. 50 °C for *rac*-BCP. Similar splittings of the chemical shift were observed in the ^{13}C NMR spectra of the ring carbons at a low temperature (e.g., -30 °C), where the rotation of the carbazole chromophore should be slow.

The RIS Analysis of NMR Data and Elucidation of Conformational Energies. Following the Flory convention,²⁸ the rotational states around the internal $\text{CH}_2\text{-CH(R)}$ bond of a vinyl chain may be designated as *t*, *g*, and \bar{g} . In the molecular system under consideration, the \bar{g} state involves very severe steric interactions arising from bulkiness of the carbazolyl group. According to Sundararajan,²² the conformation of BCP may be expressed by a 2×2 matrix scheme such as

$$U_m = \begin{bmatrix} \eta^2 \omega'' & \eta \\ \eta & \omega \end{bmatrix} \quad (1)$$

$$U_r = \begin{bmatrix} \eta^2 & \eta \omega' \\ \eta \omega' & 1 \end{bmatrix} \quad (2)$$

where suffixes *m* and *r* designate the *meso* and *racemo* configuration, respectively (Figure 2). The rows of these matrices are indexed to rotational states in the order *t* and *g* for bond 2 and the columns to those for bond 3. Sun-

Table III
Values of J_{AX} , J_{BX} , and $J_{\text{AX'}}$ Estimated for a Temperature of 300 K and the *Trans* and *Gauche* Couplings Calculated Therefrom

(a) <i>meso</i> -BCP				
solvent	J_{AX} , Hz	J_{BX} , Hz	J_{T} , Hz	J_{G} , Hz
$(\text{CD}_3)_2\text{CO}$	7.49	7.72	11.64	3.57
CDCl_3	7.65	7.68	11.73	3.60
(b) <i>rac</i> -BCP				
solvent	J_{AX} , Hz	$J_{\text{AX'}}$, Hz	J_{T} , Hz	J_{G} , Hz
$(\text{CD}_3)_2\text{CO}$	10.24	4.92	11.60	3.56
CDCl_3	11.02	4.46	11.84	3.64

dararajan's notation²² was adopted for the statistical weights. Thus, η is defined as the weight of the *t* state relative to *g*. The definition of the second-order interaction parameters is illustrated in Figure 2.

As prescribed by Bovey,²⁷ the observed vicinal coupling constants can be expressed as rotational averages of the *trans* (J_{T}) and *gauche* couplings (J_{G}). The sum, $J_{\text{AX}} + J_{\text{BX}}$ (or $J_{\text{AX'}}$) ($= J_{\text{T}} + J_{\text{G}}$), remains nearly invariant independent of temperature and solvents (cf. Tables I and II). The ratio, $J_{\text{G}}/J_{\text{T}}$, may be taken from measurements on some cyclic compounds having related chemical structures. Booth and Thornburrow²⁹ have reported values of the vicinal coupling constants $J_{1a2a} = 12.23 \pm 0.07$ and $J_{1a2e} = 3.75 \pm 0.07$ Hz for phthalimidocyclohexane and its *trans*-4-alkyl derivatives (in benzene), yielding $J_{1a2e}/J_{1a2a} \equiv J_{\text{G}}/J_{\text{T}} = 0.307$. Listed in Table III are the values of J_{AX} , J_{BX} , and $J_{\text{AX'}}$ estimated by the linear interpolation for the temperature of 300 K, and those of J_{T} and J_{G} obtained by adopting the $J_{\text{G}}/J_{\text{T}}$ ratio as mentioned above. As shown in the table, the observed results indicate $J_{\text{AX}} \approx J_{\text{BX}}$ for *meso*-BCP. The exact identification of these couplings may therefore be unimportant in this system. For *rac*-BCP, the vicinal coupling constant $^3J_{\text{CH}}$ was determined from the spectral data of the methyl carbon. The observed value (2.14 ± 0.31 Hz) is relatively small, indicating that the terminal methyl group is preferentially situated *gauche* to the methylene protons: i.e., $f_{\text{tt}} \gg f_{\text{gg}}$. The assignment of J_{AX} and $J_{\text{AX'}}$ was thus verified.

The observed coupling constants may be related to the conformational statistical weights by using eq 1 and 2:³⁰

$$(J_{\text{AX}} - J_{\text{BX}})/(J_{\text{T}} - J_{\text{G}}) = (\eta^2 \omega'' - \omega)/(\eta^2 \omega'' + 2\eta + \omega) \quad (3)$$

$$(J_{\text{AX}} - J_{\text{AX'}})/(J_{\text{T}} - J_{\text{G}}) = (\eta^2 - 1)/(\eta^2 + 2\eta \omega' + 1) \quad (4)$$

If the high-energy conformation designated with ω' is ignored, values of η may be estimated to be 2.2 in acetone- d_6 and 3.0 in CDCl_3 . The conformational energy parameters calculated by the simple Boltzmann relation $E_\eta = -RT \ln \eta$ are as follows: -0.48 (acetone- d_6) and -0.65 kcal mol⁻¹ (CDCl_3). These values are comparable to that (-0.5 kcal mol⁻¹) suggested in the conformational analysis of Sundararajan.²² In the relation derived for *rac*-BCP (eq 4), η varies rather sensitively with ω' . Sundararajan²² estimated $E_{\omega'}$ to be of the order of 0.5 kcal mol⁻¹. When $\omega' = 0.43$ (or $E_{\omega'} = -RT \ln \omega' \approx 0.5$ kcal mol⁻¹), η increases to 3.2 (acetone- d_6) and 5.2 (CDCl_3); the corresponding energies are -0.70 and -0.98 kcal mol⁻¹, respectively. As shown in Table III, the differences between J_{AX} and J_{BX} are small, and thus from eq 3,

$$\eta^2 \omega'' = \omega \quad (5)$$

In conformity with the previous argument, we estimate ω'' under two extreme conditions. For $\omega = \omega' = 0$, ω'' is also zero. If we let $\omega = \omega' = 0.43$, $\omega'' = 0.041$ (acetone- d_6) and

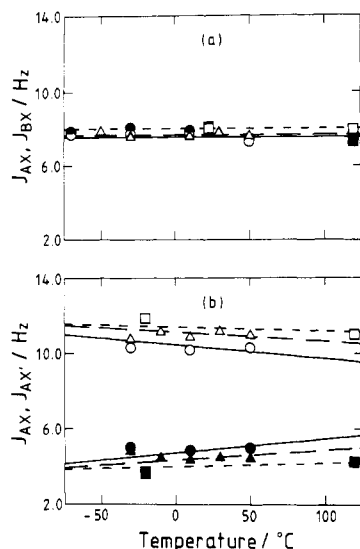


Figure 3. Comparison of calculated and observed temperature dependence of vicinal coupling constants: (a) *meso*-BCP and (b) *rac*-BCP. Observed values are indicated by circles ($(\text{CD}_3)_2\text{CO}$), triangles (CDCl_3), and squares ($n\text{-C}_8\text{D}_{18}$),²⁵ open and filled symbols being used to distinguish J_{AX} and J_{BX} (or $J_{\text{AX}'}$), respectively. Calculated results are illustrated by solid ($(\text{CD}_3)_2\text{CO}$), broken (CDCl_3), and dotted curves ($n\text{-C}_8\text{D}_{18}$).

0.016 (CDCl_3), with values of η given previously: the corresponding conformational energies are calculated to be $E_{\omega'} = 1.9$ and $2.4 \text{ kcal mol}^{-1}$, respectively. Statistical weight parameters may also be estimated from Vandendriessche et al.'s data (in $n\text{-octane-}d_{18}$)²⁵ in the same manner. The results are summarized as follows: when $\omega = \omega' = \omega'' = 0$, $\eta = 6.2$ (-1.09), and with $\omega = \omega' = 0.43$, $\eta = 18.5$ (-1.74) and $\omega'' = 0.0013$ (4.0), the values in parentheses indicating the conformational energies in kilocalorie per mole. The analysis yielded a considerably large value of η , or a large negative value of E_η . In Vandendriessche et al.'s measurements, however, the sum $J_{\text{AX}} + J_{\text{BX}}$ (*meso*-BCP) varies with temperature and consequently exceeds somewhat its counterpart $J_{\text{AX}} + J_{\text{AX}'}$ (*rac*-BCP) at 300 K. The values of the parameter set estimated above are therefore approximate.

The conformational energy parameters thus elucidated may be used to calculate the temperature dependence of the coupling constants J_{AX} and J_{BX} for *meso*-BCP and J_{AX} and $J_{\text{AX}'}$ for *rac*-BCP. The results are compared to those observed in Figure 3, where experimental data indicated by open and filled circles (acetone- d_6), triangles (CDCl_3), and squares ($n\text{-octane-}d_{18}$) are reasonably well reproduced by the respective calculations. The difference between the two parameter sets derived by setting $\omega = \omega' = 0$ and 0.43 was found to be very small for a given solvent system. These two results are therefore not distinguished in the figure.

As described above, values of J_{AX} , J_{BX} , and $J_{\text{AX}'}$ vary rather insensitively with the second-order statistical weight parameters. In view of very severe steric overlaps involved in the conformations designated with ω and ω' , the assumption such as E_ω and $E_{\omega'} > 0.5 \text{ kcal mol}^{-1}$ may be reasonable.^{16,22} Then, the present analysis leads to an estimate such as $E_\eta = -0.5$ to $-1.0 \text{ kcal mol}^{-1}$ and $E_{\omega''} > 2.0 \text{ kcal mol}^{-1}$. As mentioned above, the conformational equilibrium scheme presented by De Schryver and co-workers^{24,25} requires the entire suppression of *meso*-tt, while Sundararajan²² estimated a comparatively low energy for this state (i.e., $2E_\eta + E_{\omega''} \approx 0$). Corresponding to these two different views, two sets of parameters were chosen:

Set 1. All of the second-order interactions are of high

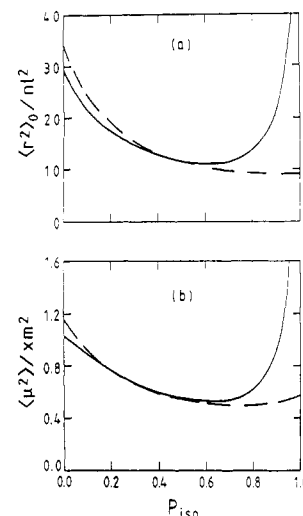


Figure 4. Configuration-dependent properties of PVK chains: characteristic ratios for (a) the mean-square end-to-end dimension and (b) the dipole moment. Calculations were performed for Monte Carlo chains of $x = 200$ units using statistical weight parameter set 1 (solid curves) and set 2 (broken curves): averages were taken over 20 chains for given values of P_{iso} .

energy, and thus $\omega = \omega' = \omega'' = 0$. The remaining parameter η is set equal to 2.5 ($E_\eta = -0.55 \text{ kcal mol}^{-1}$).

Set 2. The second-order interactions designated as ω and ω' require relatively low energy: $\omega = \omega' = 0.43$ ($E_\omega = E_{\omega'} = 0.5 \text{ kcal mol}^{-1}$). The values of η and ω'' are taken to be $\eta = 4.1$ ($E_\eta = -0.84 \text{ kcal mol}^{-1}$) and $\omega'' = 0.03$ ($E_{\omega''} = 2.0 \text{ kcal mol}^{-1}$).

The second set closely resembles that of Sundararajan ($E_\eta = -0.50$, $E_\omega = 1.1$, $E_{\omega'} = 0.50$, $E_{\omega''} = 1.0 \text{ kcal mol}^{-1}$), yet it is compatible with the results of the aforementioned NMR analysis: the difference may be noted in the statistical weights assigned to the *meso*-tt state.

Estimation of the Unperturbed End-to-End Dimension and Dipole Moment of Polymeric Chains. The RIS calculations of the characteristic ratio for the unperturbed end-to-end distance and the dipole moment were carried out by using the statistical weight parameter sets formulated in the preceding section. A conventional expression was adopted for the adjoining matrix which takes into account the neighbor-dependent character of bond rotations occurring on both sides of the methine carbon.²² The geometrical parameters used are as follows: $\text{C-C} = 1.53 \text{ \AA}$, $\angle \text{CC}^a\text{C} = 112^\circ$, and $\angle \text{C}^a\text{CC}^a = 114^\circ$ except for $\angle \text{C}^a\text{CC}^a = 117^\circ$ in the tt state. The group dipole moment is assumed to lie along the $\text{C}^a\text{-N}$ bond: $\angle \text{CC}^a\text{N} = 109^\circ$. To facilitate comparison, rotational angles were taken to be identical with those used by Sundararajan.²²

The results are shown in Figure 4, where the characteristic ratios (a) $\langle r^2 \rangle_0 / nl^2$ and (b) $\langle \mu^2 \rangle / x m^2$ are plotted as a function of P_{iso} , the replication probability of the isotactic diad. In parameter set 1, $\omega = \omega' = \omega'' = 0$, and therefore the number of chain conformations is severely limited. The isotactic chain ($P_{\text{iso}} = 1.0$) exists exclusively in one of the two equivalent helical conformations, i.e., either a left- or right-handed screw, and thus the characteristic ratios increase linearly with x . For the racemo diad, two arrangements are permitted: the weight of tt relative to gg is given by η^2 . Calculations for the syndiotactic chain ($P_{\text{iso}} = 0$) indicate that both $\langle r^2 \rangle_0 / nl^2$ and $\langle \mu^2 \rangle / x m^2$ gradually reach their asymptotic limits. The results for intermediate tacticities ($0 < P_{\text{iso}} < 1.0$) were obtained by using Monte Carlo chains of $x = 200$ units and are indicated by solid curves in Figure 4. In parameter set 2, conformational energies, E_ω and $E_{\omega'}$ are rather low. Ac-

Table IV
Bond Conformation Probabilities of *meso*- and *rac*-BCP
Estimated Using Statistical Weight Parameter Sets as
Indicated

parameter set	<i>meso</i>			<i>racemo</i>		
	tt	tg+gt	gg	tt	tg+gt	gg
set 1	0.0	1.0	0.0	0.86	0.0	0.14
set 2 ^a	0.06	0.89	0.05	0.78	0.17	0.05
Sundararajan ^b	0.10	0.87	0.03	0.70	0.19	0.11
Privratska and Havranek ^c	0.66	0.34	0.0	1.0	0.0	0.0

^a A small difference between $f_{tt,m}$ (0.06) and $f_{gg,m}$ (0.05) arises from the assignment of round numbers to the conformational energy parameters. ^b Reference 22. ^c Reference 23.

cordingly, stereochemical arrangements such as $(gg)_m$, $(tg)_r$, and $(gt)_r$ should occur readily. Occurrence of the $(tt)_m$ conformation is also enhanced, as estimated by the empirical relation (eq 5). With finite values of E_ω and $E_{\omega'}$, interruption of the helical sequence becomes probable in the perfectly isotactic chain ($P_{iso} = 1.0$). Thus, the chain acquires some flexibility, and the characteristic ratios reach their asymptotic values quite rapidly ($x < 40$). The effect of such a conformational flexibility is manifestly shown in the large decrease of $\langle r^2 \rangle_0/nl^2$ and $\langle \mu^2 \rangle/xm^2$ for highly isotactic chains (compare the solid and broken curves). In Figure 4, both $\langle r^2 \rangle_0/nl^2$ and $\langle \mu^2 \rangle/xm^2$ tend to be somewhat higher for set 2 in the syndiotactic-rich region: a difference of ca. 20% at the syndiotactic limit, i.e., $P_{iso} = 0$. In the intermediate region (e.g., $P_{iso} \approx 0.5$), the calculated values of the characteristic ratio are not much affected by an increase of $\omega = \omega' = 0$ to 0.43. Experimental values of $\langle r^2 \rangle_0/nl^2 = 15\text{--}19$ and $\langle \mu^2 \rangle/xm^2 = 0.3\text{--}0.5$ were derived for samples having tacticities (P_{iso}) ranging approximately from 0.3 to 0.5. For these experimental results, parameter sets 1 and 2 are equally favorable (Figure 4). Sundararajan deduced his parameter set by comparing the calculated values of $\langle r^2 \rangle_0/nl^2$ with those observed. The conformational energy parameters determined in this manner, especially $E_{\omega'}$, should be less reliable.

The observed enhancement in $\langle r^2 \rangle_0/nl^2$ as compared with the other vinyl polymers such as polystyrene³¹ may be due to a large negative value of E_η rather than the difference in the $E_{\omega'}$ values.²²

Elucidation of Bond Conformations. The statistical weight parameter sets examined in the preceding section may be used to estimate bond conformation probabilities along a given chain. The results of the analysis on *meso*- and *rac*-BCP are listed in Table IV, where fractions derived by using the parameter set of Sundararajan²² as well as that of Privratska and Havranek²³ are included for comparison. With an increase in ω and ω' (or a decrease in the corresponding conformational energies), the most preferred conformations, i.e., *meso*-tg and *racemo*-tt, tend to be reduced (compare sets 1 and 2). Populations of the *meso*-tt and *racemo*-tg forms are enhanced when Sundararajan's set²² is used. Especially, an increase of *meso*-tt from 0.06 (set 2) to 0.10 (Sundararajan's set) is significant. This difference amounts to a decrease of 0.5 kcal mol⁻¹ in E_ω ($=2E_\eta + E_{\omega'}$) in parameter set 2. For *meso*-BCP, $f_{tt} \approx f_{gg}$ is the requirement from the ¹H NMR observation. In this regard, the parameter sets of Sundararajan as well as Privratska and Havranek are incompatible with experimental observations. Use of the parameter set derived from Vandendriessche et al.'s NMR data,²⁸ characterized by a large value of η , yields a distribution in favor of the tt conformation in both *meso*- and *rac*-BCP. As pointed out previously, however, the coupling constants obtained in their measurements involve some inconsistency. The results are therefore not shown explicitly.

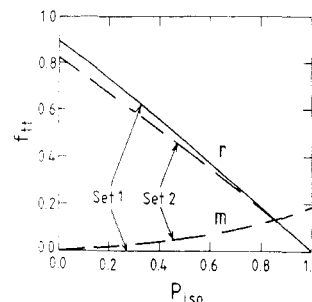


Figure 5. Fractions of the tt conformation for the *meso* (m) and *racemo* diad (r) occurring in PVK chains, calculated for $x = 200$ units by using statistical weight parameter set 1 (solid curves) and set 2 (broken curves): averages were taken over five chains for given values of P_{iso} .

In the photophysical process of the PVK system, the tt conformations seem to play the most important role.³² As is exhibited in the chemical shift difference of the ring protons, relative orientation of the neighboring carbazolyl groups is somewhat different between the *meso*-tt and *racemo*-tt forms. Fractions of these tt states were separately estimated for Monte Carlo chains comprising $x = 200$ units. The results are illustrated in Figure 5 as a function of P_{iso} . Since $\omega'' = 0$ in set 1, the *meso*-tt state is not permitted, and thus, $f_{tt,m} = 0$ for all values of P_{iso} . With $\omega'' = 0.43$ (set 2), the value of $f_{tt,m}$ increases to 0.19 for the perfectly isotactic chain. This value is substantially larger than the corresponding value (0.06) calculated for *meso*-BCP. Such an enhancement in $f_{tt,m}$ arises from the neighbor-dependent character of the bond rotation of the vinyl-type polymer chain.³³ For a given parameter set, the sum of two curves, $f_{tt,m} + f_{tt,r}$, gives the total tt fraction of the chain. At $P_{iso} = 0.5$, for example, the value of $f_{tt,m} = 0$ (set 1) to 0.05 (set 2), while $f_{tt,r} = 0.47$ (set 1) to 0.43 (set 2). For comparison, use of the statistical weight parameters assembled by the other research groups gave the following results at $P_{iso} = 0.5$: $f_{tt,m} = 0.08$ and $f_{tt,r} = 0.40$ (Sundararajan²²); $f_{tt,m} = 0.27$ and $f_{tt,r} = 0.50$ (Privratska and Havranek²³).

As noted in the excimer fluorescence studies, the *meso*-tt form, having the so-called sandwich structure, is one of the major species responsible for the emission spectrum.^{24,25,32} In the excited state, formation of the tt form is very rapid. The exciton-resonance interaction is suggested as a possible cause of the large stabilization energy required in this conformation.³⁴ In the excited state, the stereochemical configuration of the PVK chain should be quite different from those depicted according to the ground-state statistics.

Conclusion

In this work, probable ranges of the conformational energy parameters were estimated by utilizing the information provided by the ¹H NMR analysis on the dimer model compounds. It should be emphasized that the NMR data of BCP can be reconciled with the RIS scheme adopted for usual vinyl polymers without assuming any particular model such as that proposed by De Schryver and co-workers. As discussed in the text, however, there still remains some ambiguity in the determination of the second-order interaction parameters, i.e., $E_{\omega'}$'s. In consideration of the E_ω values adopted in the analysis of the other vinyl polymer chains such as polystyrene,³¹ the values of E_ω and $E_{\omega'}$ may be of the order of 2 kcal mol⁻¹: then values of $E_\eta = -0.6 \pm 0.1$ and $E_{\omega'} = 3.2 \pm 0.2$ kcal mol⁻¹ follow from the NMR data as analyzed by the relations given in eq 3-5. With these conformational energies, we obtain

$\langle r^2 \rangle_0 / nl^2 = 25.3$ and $\langle \mu^2 \rangle / xm^2 = 1.3$ for a perfectly isotactic chain ($P_{iso} = 1.0$).

Registry No. PVK, 25067-59-8; BCP, 102197-47-7.

References and Notes

- Heller, J.; Tieze, D. O.; Oarkinson, D. B. *J. Polym. Sci., Part A* **1963**, *1*, 125.
- Yoshimoto, S.; Akana, Y.; Kimura, A.; Hirata, H.; Kusabayashi, S. *J. Chem. Soc. D* **1969**, 987.
- Williams, D. J. *Macromolecules* **1970**, *3*, 602.
- Okamoto, K.; Yamada, M.; Itaya, A.; Kimura, T.; Kusabayashi, S. *Macromolecules* **1976**, *9*, 645.
- Griffiths, C. H. *J. Polym. Sci., Polym. Lett. Ed.* **1978**, *16*, 271.
- Williams, D. J.; Froix, M. F. *Polym. Prepr. (Am. Chem. Soc., Div. Polym. Chem.)* **1977**, *18*, 445.
- Kawamura, T.; Matsuzaki, K. *Makromol. Chem.* **1978**, *179*, 1003.
- Kawamura, T.; Matsuzaki, K. *Makromol. Chem.* **1981**, *182*, 3003.
- Terrell, D. R.; Evers, F. *Makromol. Chem.* **1982**, *183*, 863.
- Terrell, D. R.; Evers, F. *J. Polym. Sci., Polym. Chem. Ed.* **1982**, *20*, 2529.
- Kawamura, T.; Sakuma, M.; Matsuzaki, K. *Makromol. Chem., Rapid Commun.* **1982**, *3*, 475.
- Sitaramaiah, G.; Jacobs, D. *Polymer* **1970**, *11*, 165.
- Kuwahara, N.; Higashida, S.; Nakata, M.; Kaneko, M. *J. Polym. Sci., Polym. Phys. Ed.* **1969**, *7*, 285.
- Leon, L. M.; Katime, I.; Rodriguez, M. *Eur. Polym. J.* **1979**, *15*, 29.
- Urizar, M.; Rodriguez, M.; Leon, L. M. *Makromol. Chem.* **1984**, *185*, 765.
- Flory, P. J. *Statistical Mechanics of Chain Molecules*; Interscience: New York, 1969.
- Beevers, M. S.; Mumby, S. J. *Polym. Commun.* **1984**, *25*, 173.
- Mumby, S. J.; Beevers, M. S. *Polymer* **1985**, *26*, 2014.
- Molina, M. S.; Barrales-Rienda, J. M.; Riande, E. *Macromolecules* **1984**, *17*, 2728.
- Baysal, B. M.; Aras, L. *Macromolecules* **1985**, *18*, 1693.
- North, A. M.; Phillips, P. J. *Chem. Commun.* **1968**, 1340.
- Beevers et al.¹⁷ measured the dipole moment of *N*-ethylcarbazole as a model compound for PVK. The observed value of 2.08 D is substantially lower than that (2.96 D) of *N*-isopropylcarbazole reported by North et al.²⁰ If we adopt the former value for *m*, the dipole moment ratios estimated in the text should be nearly doubled.
- Sundararajan, P. R. *Macromolecules* **1980**, *13*, 512.
- Privratska, J.; Havranek, A. *Acta Polym.* **1980**, *31*, 130.
- De Schryver, F. C.; Vandendriessche, J.; Toppet, S.; Demeyer, K.; Boens, N. *Macromolecules* **1982**, *15*, 406.
- Vandendriessche, J.; Palmans, P.; Toppet, S.; Boens, N.; De Schryver, F. C.; Masuhara, H. *J. Am. Chem. Soc.* **1984**, *106*, 8057.
- Evers, F.; Kobs, K.; Memming, R.; Terrell, D. R. *J. Am. Chem. Soc.* **1983**, *105*, 5988.
- Bovey, F. A. *High Resolution NMR of Macromolecules*; Academic: New York, 1972. Bovey, F. A.; Hood, F. P.; Anderson, E. W.; Synder, L. C. *J. Chem. Phys.* **1965**, *42*, 3900.
- Flory, P. J.; Sundararajan, P. R.; DeBolt, L. C. *J. Am. Chem. Soc.* **1974**, *96*, 5015.
- Booth, H.; Thornburrow, P. R. *J. Chem. Soc. B* **1971**, *2*, 1051.
- Moritani, T.; Fujiwara, Y. *J. Chem. Phys.* **1973**, *59*, 1175.
- Yoon, D. Y.; Sundararajan, P. R.; Flory, P. J. *Macromolecules* **1975**, *8*, 776.
- Masuhara, H.; Vandendriessche, J.; Demeyer, K.; Boens, N.; De Schryver, F. C. *Macromolecules* **1982**, *15*, 1471. Masuhara, H.; Tamai, N.; Mataga, N.; De Schryver, F. C.; Vandendriessche, J. *J. Am. Chem. Soc.* **1983**, *105*, 7256. Masuhara, H.; Tamai, N.; Mataga, N.; De Schryver, F. C.; Vandendriessche, J.; Boens, N. *Chem. Phys. Lett.* **1983**, *95*, 4-5, 471.
- Abe, A. *J. Am. Chem. Soc.* **1968**, *90*, 2205; *Polym. J.* **1970**, *1*, 232; *Macromolecules* **1977**, *10*, 34.
- Padma, Malar, E. J.; Chandra, A. K. *Theor. Chim. Acta* **1980**, *55*, 153.

Photoinduced Conformational Transition of Polypeptide Membrane Composed of Poly(L-glutamic acid) Containing Pararosaniline Groups in the Side Chains

Morimasa Sato, Takatoshi Kinoshita,* Akira Takizawa, and Yoshiharu Tsujita

Department of Materials Science & Engineering, Nagoya Institute of Technology, Gokiso-cho, Showa-ku, Nagoya 466, Japan. Received February 24, 1988; Revised Manuscript Received May 11, 1988

ABSTRACT: Photoresponsive polypeptide membranes have been prepared by casting a dimethylformamide solution of poly(L-glutamic acid) (PGA) containing ca. 10 mol % pararosaniline (rose) groups in the polymer side chains (rose-PGA). The dark-adapted rose-PGA membranes in the aqueous solution exhibited a unique CD pattern with the pH dependence of the secondary structure, suggesting loss of α -helix structure at low and high pHs and formation of helix near weak alkaline pH. This behavior arises from the amphoteric nature of the rose-PGA side chains; i.e., the L-glutamic acid moiety is negatively charged at high pH, whereas the rose moiety is positively ionized at low pH. The light irradiation of the rose-PGA membranes produced changes in the secondary structure of the membranes, random coil to helix and helix to random coil transitions, depending on the pH at which the irradiation was carried out. The induced conformational transitions of the membrane can be explained in terms of the photoinduced changes in the balance of electrostatic interactions between oppositely charged side chains, based on a cooperative effect between the photodissociation of the rose moiety with production of a hydroxide ion and the induced acid dissociation of L-glutamic acid moiety accompanied by the increase in pH in the membrane phase on UV irradiation. After removal of the light, rose-PGA in the membrane returned to the initial conformation after 100 min in the dark.

Recently, many biological studies provide evidence that living cells have systems for information reception, intracellular transmission, and transduction and/or response along the route of signal transmission. It has been rec-

ognized, for example, that photoreceptors translate the information accepted by rhodopsin into transmembrane photoreceptor potentials resulting from conformational changes of channel proteins. In the vertebrate photosen-